Chapter 2

Literature Review

2.1 Introduction

This chapter presents the literature studies in relation to the works done for this research. The study begins with a brief preview on silicon carbide as the research material. This is followed by studies done by other researchers on the structural and optoelectronic properties of silicon carbide thin films using various deposition techniques. Focus of literature is on the issues regarding the utilization of various chemical vapor deposition techniques in preparing silicon carbide thin film. Studies also include the role of hydrogen in the crystallization of silicon carbide. Stress on this chapter is put upon the development of the film microstructure with regards to deposition parameters and techniques.

2.2 A Preview on Silicon Carbide

Silicon carbide is a versatile material utilized in a wide variety of applications. Starting as a durable hardware material, silicon carbide purposes had stretched to nanoscale electronic devices. Later, its application to carbonaceous compounds studied by E.G. Acheson in 1891 had made silicon carbide came into focus. It was said that Acheson was trying to dissolve carbon in molten corundum (alumina) when he discovered the presence of hard, blue-black crystals which he believed to be a compound of carbon and corundum and thus called it carborundum. Acheson found that the material formed in the furnace varies in purity according to its distance from the heat source. The products were mainly crystalline and were characterized by great hardness, refractability and infusibility.

Naturally, silicon carbide is mainly a chemical compound that forms hard, dark and iridescent crystals that are insoluble in water and other common solvents. It is widely used as an abrasive under more familiar names such as Carborundum and

Crystolon. As silicon carbide only decomposed when heated up to about 2700^{o}C, it is widely known as a heat resistant material. In hardware industry, its versatility includes several applications in refractory materials such as rods, tubes, fire-brick and in certain parts of nuclear reactors. Silicon carbide can also exist in the form of fibers and are added as reinforcement to plastics and light metals to increase strength and stiffness.

Investigations on the electronic properties of silicon carbide started in early 1900. Electroluminescence of silicon carbide was observed by Captain Henry Joseph Round in 1907 and later by O.V. Losser in 1923. It was in 1907 when silicon carbide was used to make the first light emitting diode (LED). The first commercial device for SiC was the blue LED (Zeigler *et al.*, 1983). In 1955, a new concept of growing high quality crystals was discovered by Lely (Lely, 1955). The research in silicon carbide then became more intensified and the first conference on silicon carbide was held in Boston in 1958. However, the interest in silicon carbide has declined in the west until the year 1978. Since then, silicon carbide has been a favorable device due to excellent performances when operating at high temperature, high power and high frequencies. Its physical and electronic properties such as wide band gap, high critical electric field, high thermal conductivity and high saturation velocity of carriers are the focus among researchers for many decades. However, besides high temperature operation at above 500 K and applications in the blue and ultraviolet region, optoelectronic applications of silicon carbide were rather limited due to the fact that all silicon carbide polytypes are indirect semiconductors. In certain aspects, the performances of silicon carbide devices did not exceed those of Si or GaAs devices (Ruff, Mitlehner and Helbig, 1994).

2.3 Some Applications of Silicon Carbide

In the semiconductor industry, silicon carbide is one of the oldest and promising materials used in preparation of semiconductors. Hydrogenated amorphous silicon carbide (a-SiC:H) improves the efficiency of amorphous silicon solar cells when used as a window layer due to its wide band gap. Being a material of good commercial value, silicon carbide is commonly manufactured by fusing sand and carbon in electric furnaces at temperatures between 1600 to 2500^{o}C. Of all its polytypes, the most commonly produced is alpha silicon carbide (α-SiC), which is formed at temperatures above 2000^{o}C and has the typical hexagonal crystal structure. Another modification of silicon carbide, the beta silicon carbide (β-SiC) which has a face-centered cubic crystal structure is formed at temperatures below 2000^{o}C.

Silicon carbide is widely used as blue LEDs, ultrafast Schottky diodes, ultraviolet detector and MESFETs. Its wide band gap, polytypism and high thermal resistance has enabled it to operate in severe environments such as high voltages, high frequencies and high temperatures. Silicon carbide is also used as substrate for other semiconductor materials due to its high thermal conductivity. Silicon carbide crystals are used in semiconductors for high temperature applications where it is highly conductive. Hydrogenated amorphous silicon carbide (a-SiC:H) with wide energy band gaps above 2.0 eV is an important material for amorphous-silicon-based solar cells. Pure α-SiC is an intrinsic semiconductor with energy band gap of 3.26 eV for 4H polytype and 3.00 eV for 6H polytype. Some physical properties of silicon carbide are listed in Table 2.1 (Jacobs and Thomas, 2005).

Nanocrystalline cubic silicon carbide (nc-3C-SiC) is also a wide band gap material and has attracted much attention as window layer of Si-based thin film solar cells (Banerjee *et al.*, 2007 and Ogawa *et al.*, 2007). As a semiconductor, silicon carbide

quantum dots are good candidates to build nanostructure photoluminescence materials for semiconductor-based ultraviolet and blue light sources.

Table 2.1: Physical properties of silicon carbide.

Property	**Value**
Melting point	2800^{o}C (approximately)
Maximum Service Temperature	2589 K
Density	3210 kg/m^3
Specific Gravity	3.2 g/cm^3
Coefficient of Thermal expansion	4.3 x 10^{-6} m/m/K
Modulus of Elasticity	65.5 x 10^4 MPa
Hardness	9 Mohs

The first semiconductor device exhibiting transistor action was developed in 1947 and was based on germanium (Ge). Even though germanium has electron mobility twice that of silicon (Si), the native oxide on germanium is unstable due to low melting point and is susceptible to moisture. Furthermore, the low band gap of germanium has prevented it from playing an important role in semiconductor technology. Therefore silicon remains the dominant material for most electronic device applications. Although indirect wide band gap semiconductors such as silicon carbide and diamond are not suitable for optoelectronic applications, they are strong candidates for power applications and high temperature applications where silicon cannot be used due to its relatively small band gap of 1.1 eV. This is because low energy band gap leads to transitions in doped semiconductors towards intrinsic behavior at relatively low temperatures and thus a loss of the dominant n- or p-type behavior (Askeland and Phule, 2004).

2.4 Silicon Carbide Structure

Materials can be categorized as either crystalline or amorphous. If the materials' atoms are arranged in a periodic fashion, it is categorized as crystalline material. Amorphous materials include materials at which the material's atoms do not have a long-range order (LRO). A material displays short-range order (SRO) if the special arrangement of the atoms extends only to the atoms' nearest neighbors. Examples of SRO materials are water (H_2O) and organic glasses.

Most metals and alloys, semiconductors, ceramics, and some polymers have a crystalline structure in which the atoms or ions display long-range order (LRO), at which, the special atomic arrangement extends over much larger length scales (>100nm) or. The atoms or ions in these materials form a regular repetitive, grid-like pattern, in three dimensions and referred to as crystalline materials. If the crystalline material consists of only one large crystal, it is referred to as a single crystal material. Single crystal materials are useful in many electronic and optical applications. A poly-crystal material is comprised of many small crystals with varying orientation in space. These smaller crystals are known as grains. The borders between tiny crystals where the crystals are in misalignment are known as grain boundaries. Many crystalline materials in engineering applications are polycrystalline.

The properties of polycrystalline materials depend upon the physical and chemical characteristics of both grains and grain boundaries. The properties of single crystal materials depend upon the chemical composition and specific directions within the crystal, known as the crystallographic direction.

Silicon carbide is a wide band gap semiconductor of greater than 2.4 eV that does not occur as a mineral. It is produced synthetically. Its crystalline structure is diamond-like, with alternating Si and C atoms covalently bonded together to produce a

material that is almost as hard as diamond. Very pure silicon carbide is colorless. Silicon carbide crystals fracture in a way that leaves them with sharp edges. These properties make silicon carbide an important industrial abrasive.

Silicon carbide crystals are also used in semiconductors for high temperature applications. Silicon carbide crystallizes in different polytypes. Polymorphysm refers to the possibility of an element or compound to crystallize in different structures. Polytypes only differ for the stacking sequence of atomic layers along one crystalline direction. In silicon carbide, the basic units are tetrahedrous with a carbon, C(Si) atom at the center, covalently bonded to four surrounding silicon, Si(C) atoms. These units are periodically repeated in closed-packed hexagonal layers, whose stacking sequence gives rise to the different polytypes. Diagram of several silicon carbide polytypes are shown in Figure 2.1 and Figure 2.2. The polytypes show a similar local chemical environment for both the carbon and silicon species although being different in the long range order. In particular, each C(Si) atom is situated above the center of a triangle of Si(C) atoms and underneath a Si(S) atom belonging to the next layer in a tetrahedral coordination. The distance between neighboring Si or C atoms is approximately 3.08 Å, while the distance between the C atoms to each of the Si atoms (Si-C bond length) is roughly equal to 1.89 Å for all polytypes. Table 2.2 shows the lattice parameters of several silicon carbide polytypes at 300 K (Harris *et al.*, 1995). Despite the many polytypes, only a few polytypes (4H, 6H, 3C) are of technological interest and the 3C cubic polytype can be grown on silicon substrate. The growth of silicon carbide on silicon substrate is of particular interest as silicon is relatively an inexpensive substrate material and all process technologies are well established.

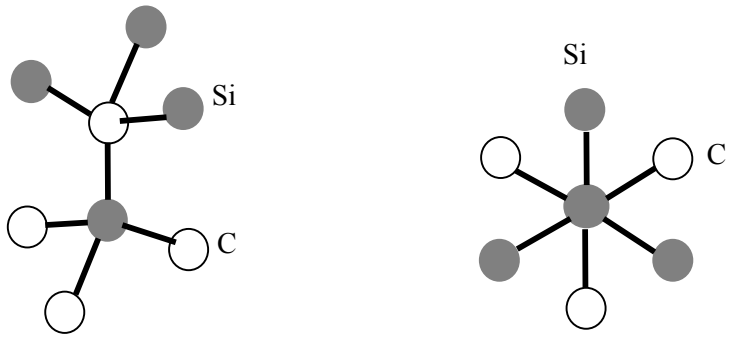

(a) Side view (b) Top view

Figure 2.1: Elementary cubic structure of silicon carbide.

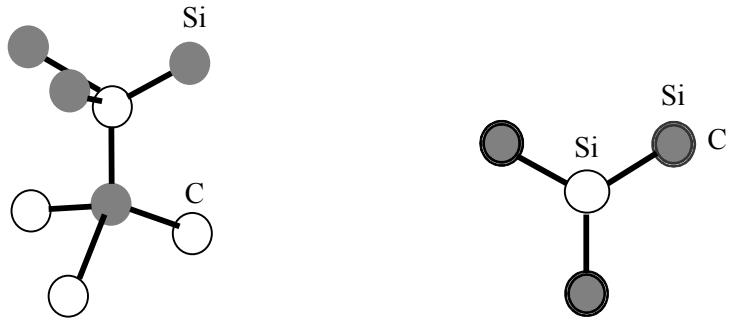

(a) Side view (b) Top view

Figure 2.2: Elementary hexagonal structure of silicon carbide.

The amorphous phase of silicon carbide is of practical importance due to its adjustable silicon (Si) and carbon (C) stoichiometry. In electronic applications, any chemical disorder can have a dramatic impact on electronic structure. Thus the stoichiometry of amorphous silicon carbide clusters indicative of Si-Si and C-C bonds is a critical metric to compare to the performance. In studies done by Swain and Dusane (2006) on the multiphase structure of hydrogen diluted amorphous silicon carbide (a-SiC:H) deposited by HW-CVD, they reported that broad peaks observed between 25^{o} and 30^{o} and 42^{o} and 50^{o} in the XRD spectra which confirmed that there is no long range

ordering in the prepared a-SiC:H films. The absence was due to strong intermediate range order established in the cluster of Si-C, C-C or Si-Si. Table 2.3 provides the bonding energy between silicon atom and some other materials (Sachdev and Scheid, 2001).

Table 2.2: Lattice parameters of several silicon carbide polytypes (Harris, 1995).

Polytype	Lattice parameters
3C	a = 4.3596
2H	a = 3.0763; c = 5.0480
4H	a = 3.0730; c = 10.053
6H	a = 3.0806; c = 15.1173
15R	a = 12.691; $\alpha = 15^{o}54'$
21R	a = 17.683; $\alpha = 9^{o}58'$

Table 2.3: Bonding energy of some related materials.

	Bonding Energy (kJ/mol)
Silicon-Silicon, Si-Si	222*
Silicon-Carbon, Si-C	275**
Silicon-Carbon, Si-C	306*
Silicon-Hydrogen, Si-H	326**
Silicon-Chlorine, Si-Cl	398*
Silicon-Nitrogen, Si-N	335*
Silicon-Oxygen, Si-O	375***
Carbon-Hydrogen, C-H	416*
Carbon-Hydrogen, C-H	435***
Carbon-Carbon, C-C	345*
Carbon-Carbon, C-C	370***
Carbon-Carbon, C=C	615*
Carbon-Carbon, C=C	680***
Carbon-Carbon, C≡C	890***

References:
*Sachdev and Scheid (2001).
**Dua *et al.* (2004).
***Smith and Hashemi (2006).

In the study of silicon carbide physical structure, the significance of grain size is not negligible. The average grain size is often closely related to the primary particle size. An exception to this is if there is grain growth due to long sintering times or exaggerated or abnormal grain growth. Typically, ceramics with a small grain size are stronger than coarse-grained ceramics. Finer grain sizes help reduce stress that develop at grain boundaries due to anisotropic expansion and contraction. Magnetic, dielectric and optical properties of ceramic materials depend upon the average grain size, and in these applications, grain size must be controlled properly. In certain applications, it is important to use single crystals of ceramic materials so as to avoid the deleterious grain boundaries that are always present in polycrystalline ceramics.

The chemical reactions in a chemical vapor deposition process can be either homogeneous or heterogeneous. Homogeneous reactions occur in the gas phase while heterogeneous reactions occur at the substrate surface. Table 2.4 provides a list of the most profound reactions for both Si and C species.

2.4.1 Utilizing Fourier-Transformed Infra-Red Spectroscopy

Carbon incorporation and the formation of silicon carbide in the films are indicated in the Fourier-Transformed Infra-Red (FTIR) spectra of the films. The major absorption bands observed are in the region 2800-3000, 2000-2100, 960-1100 and 740-800 cm^{-1}. The band corresponding to 2800-3000 cm^{-1} is attributed to the stretching vibration of CH_n groups in sp^2 (2880 cm^{-1}) and sp^3 (2960 cm^{-1}) configurations, while that at 2000-2100 cm^{-1} is attributed to the stretching vibration of SiH_n groups. The band at 960-1100 cm^{-1} corresponds to CH_n wagging or bending modes while the strong band at 780 cm^{-1} corresponds to the Si-C stretching mode (Kumbhar *et al.*, 2001). The

chemical bonds that exist in the silicon carbide films prepared in this work in accordance to the FTIR absorptions peaks are listed in Table 2.5.

It was also reported that small bands occur at 880 cm^{-1} and 650 cm^{-1} for films deposited at C_2H_2 fraction less than 0.67 (Kumbhar *et al.*, 2001). These correspond to SiH_2 bending and SiH_n wagging modes respectively. These bands are absent for films deposited at higher C_2H_2 fractions. The shift of the 2100 cm^{-1} Si-H stretching peak could be attributed to two factors. The factors could either be the $(SiH_2)_n$ formation in microvoids; or the nearest neighbor silicon atoms are progressively replaced by carbon, oxygen or nitrogen atoms. It is also observed that in spite of the decrease in Si-C bonding with an increase in the fraction beyond 0.67, the optical band gap tends to increase, and reaches a maximum of 3.5 eV at C_2H_2 fraction of 0.8 (Kumbhar *et al.*, 2001). They believe that the increase in the band gap is due to the increase in the sp^3-bonded CH_n observed at 960 cm^{-1}.

In the FTIR spectra, the presence of $Si\text{-}CH_3$ bending mode and $Si\text{-}CH_3$ asymmetric deformation in the wave number range of 1300 to 1500 cm^{-1} and CH, CH_2 and CH_3 stretching modes in 2800 to 3000 cm^{-1} wave number range indicates significant amount of carbon incorporation into the films (Das, Chattopadhyay and Barua, 1998, King *et al.,* 2011).

Ferreira *et al.* (2002) observed that the area and the intensity of the SiC peak increases as the C_2H_4 in the gas mixture increases, revealing an enhancement of carbon incorporation into the films. On the other hand, increase in the intensity of the SiC peak is accomplished by a decrease in the area of SiH_x vibration mode. The relation between the areas of SiH_x wagging and SiC stretching peaks $A^w{}_{SiHx}/A^s{}_{SiC}$ was observed in their work.

By using DC magnetron sputtering technique, Keffous *et al.* (2010) syntesized a-$Si_{1-x}C_x$:H films and reported FTIR absorptions for the following; 512 cm^{-1} and 769 cm^{-1} for Si-C wagging mode and transitional phase respectively, 660 cm^{-1} for Si-Si stretching vibration, 1108 cm^{-1} for Si-O-Si and 2069 cm^{-1} for Si-H. Here, the Si-Si absorption band is due to the silicon substrate.

Table 2.4: List of the most profound reactions for Si and C species.

Homogeneous reaction	**Heterogeneous reaction**
Si species	
$SiH_4 \longleftrightarrow SiH_2 + H_2$	$Si\ (g) \longleftrightarrow Si\ (s)$
$Si + H_2 \longleftrightarrow SiH_2$	$SiH_2\ (g) \longleftrightarrow Si\ (s) + H_2\ (g)$
$SiH_2 + Si \longleftrightarrow Si_2H_2$	$Si_2H_2\ (g) \longleftrightarrow 2Si\ (s) + H_2\ (g)$
$Si_2 + H_2 \longleftrightarrow Si_2H_2$	
C species	
$C_3H_8 \longleftrightarrow CH_3 + C_2H_5$	$C_2H_4\ (g) \longleftrightarrow 2C\ (s) + 2H_2\ (g)$
$CH_3 + H_2 \longleftrightarrow CH_4 + H$	$C_2H_2\ (g) \longleftrightarrow 2C\ (s) + H_2\ (g)$
$2C_2H_5 \longleftrightarrow 2C_2H_4 + H_2$	$CH_4\ (g) \longleftrightarrow C\ (s) + 2H_2\ (g)$
$C_2H_4 \longleftrightarrow C_2H_2 + H_2$	

Table 2.5: Signatures of chemical bonds identified in the silicon carbide films prepared in this work.

Bond Structure	**Mode**	**Wavenumber(cm^{-1})**	**References**
Si- entities			
Si-H_n	Rocking	620, 640	Wang, Yue and Liu (2002).
Si-H_n	Wagging	650	Tabata *et al.* (2004).
Si-H_n	Wagging	650	Kumbhar *et al.* (2001).
Si-H_2	Bending	880	Kumbhar *et al.* (2001).
Si-H_2, Si-H_3	Bending	890	Wang, Yue and Liu (2002).
Si-H_n groups	Stretching	2000-2100	Kumbhar *et al.* (2001).
Si-H_n (n=1,2)	Stretching	2000-2200	Kaneko *et al.* (2005).
Si-H	Stretching	2030-2080	Wang, Yue and Liu (2002).
Si-H	Stretching	2113	Yu *et al.* (2000).
Si-C	Stretching	750	Wang, Yue and Liu (2002).
Si-C	Stretching	780	Kumbhar *et al.* (2001).
Si-C	Stretching	790	Kaneko *et al.* (2005).
Si-C	Stretching (mode in crystalline phase)	794	Yu *et al.* (2000).
Si-CH_3	Wagging	780	Tabata *et al.* (2004).
Si-CH_2 Si-CH_3	Bending	1000	Tabata *et al.* (2004).
Si-CH_2 Si-CH_3	Rocking	1250	Wang, Yue and Liu (2002).
Si-CH_3	Bending	1250	Kaneko *et al.* (2005).
Si-CH_3	Bending/ Asymmetric deformation	1300 to 1500	Das, Chattopadhyay and Barua (1998).
Si-O-Si	Stretching	1100	Wang, Yue and Liu (2002).

Bond Structure	**Mode**	**Wavenumber(cm^{-1})**	**References**
C- entities			
$C-H_n$	Wagging/ Bending	960-1100	Kumbhar *et al.* (2001).
$C-H_n$	Rocking or Wagging	980	Tabata *et al.* (2004).
$C-H_2$	Wagging	1000	Kaneko *et al.* (2005).
C-H	Rocking or Wagging (due to high concentration of H_2)	1008	Yu *et al.* (2000).
$C-H_2$	Bending	1030	Yu *et al.* (2000).
C-CH	Bending	1400	Yu *et al.* (2000).
Regions of access C having a crystalline graphite structure		1644	Yu *et al.* (2000).
C-H, $C-H_2$ and $C-H_3$	Stretching	2800 to 3000	Das, Chattopadhyay and Barua (1998).
$C-H_n$ groups in sp^2	Stretching	2880	Kumbhar *et al.* (2001).
$C-H_2$	Stretching	2890	Kaneko *et al.* (2005).
C-H	Stretching	2927	Yu *et al.* (2000).
$C-H_n$ groups in sp^3	Stretching	2960	Kumbhar *et al.* (2001).
$C-H_3$	Stretching	2960	Kaneko *et al.* (2005).

2.4.2 Utilizing Raman Spectroscopy

Raman spectroscopy is based on the Raman scattering phenomenon of electromagnetic radiation by molecules (Leng, 2008). When materials are irradiated with electromagnetic radiation of single frequency, the light will be scattered by molecules both elastically and in-elastically. Elastic scattering means that the scattered light has the same frequency as that of the radiation. Inelastic scattering means that the scattered light has a different frequency from that of the radiation. Elastic scattering is called Rayleigh scattering while inelastic scattering is called Raman scattering. Both elastic and inelastic can be understood in terms of energy transfer between photons and molecules.

Micro-Raman Spectroscopy is done in order to investigate the molecular vibration frequency which corresponds to the frequency changes caused by the scattering by molecules. Raman scattering is a useful, sensitive, precise, and non-destructive technique for the characterization and study of semiconductor materials. Raman characterization can give an indication of the degree of the crystalline structure of the CVD-grown films. However, the amount of crystalline volume fraction of μc-SiC:H films can not be evaluated from the Raman spectra in a similar way like in μc-Si:H (Chen *et al.*, 2009 and Hong *et al.,* 2010). Therefore, the crystalline volume fraction of their μc-SiC:H films was estimated by the ratio of Lorentzian-to-Gaussian contribution (I^{IR}_C) in the infrared absorption line of the Si-C stretching mode at 800 cm^{-1} as $I^{IR}_C = A_L/(A_L + A_G)$, where A_L and A_G refer to the Lorentzian peak area and Gaussian peak area respectively.

The structure of silicon carbide can also be studied using the Raman spectra. Tung *et al.* (2005) decomposed ethylene on silicon wafer using hot filament CVD method at low substrate temperature of 200^{o}C. The appearance of wide peaks around

480 cm^{-1} and 750-800 cm^{-1} in the Raman spectra suggests that there are separated a-SiC clusters in the films. Wideness and shift of that peak depend on the percentage of Si-C in the films (Shi *et al.*, 1999) and the size of Si-C clusters or grains. The widening of the peaks in the spectra can be related to complicated chemical composition and in homogeneous structure of film as well as superposition of different spectral modes from different components.

Feng *et al.* (1998) suggests that a 20% misfit between Si and 3C-SiC is the main reason for the difficulty of the growth of SiC on Si. Their Raman studies on 3C-SiC showed an average in-plane strain in the 3C-SiC films which is far smaller than what might have been expected from a 20% mismatch The Raman signal from the Si substrate is enhanced by the epitaxy of a CVD 3C-SiC film and is reduced by the deposition of a very thin layer of amorphous SiC. The 3C-SiC Raman phonons from SiC/Si are enhanced upon removal of the Si substrate and different selection rule are operable due to the difference between the SiC-Si interface and the SiC-air interface.

In their work where hydrogenated nanocrystalline Silicon Carbide is synthesized by ECR-CVD, Yu *et al.*(2000) reported three main peaks at 785.3 cm^{-1}, 986.4 cm^{-1} and 1606 cm^{-1}, and a weak shoulder peak at approximately 1390.2 cm^{-1} in their Raman spectra. The peak at 1606.5 cm^{-1} and its weak shoulder at 1390.2 cm^{-1} correspond to the characteristic G-peak and D-peak of disordered graphite respectively. The 785.3 cm^{-1} and 986.4 cm^{-1} peaks are corresponded to longitudinal and transverse optical phonons of crystalline SiC respectively.

Swain and Dusane (2006) observed crystalline-Si Raman mode and a second-order Raman band (which was attributed to silicon substrate) at 521 cm^{-1} and 970 cm^{-1} respectively, besides (first-order scattering) amorphous Si-Si Raman mode at 475 cm^{-1}. They reported that C-C bands were increased by increasing H_2 flow rate, indicating the

presence of amorphous-Si in Si-rich a-SiC:H thin films. Low Raman efficiencies of the Si-C bands have resulted in weak 600-1000 cm^{-1} band. The Raman band for C-C bonds in the region of 1300-1600 cm^{-1} which was not detected indicated low C-C bond concentration in the film. The weak C-C band also indicated that the hydrogenated amorphous silicon carbide (a-SiC:H) thin film was almost stoichiometric.

In their studies on the structural and optical properties of hydrogenated amorphous silicon carbide (a-SiC:H), Yu *et al.* (2004) observed five vibration bands in the Raman spectra for their Si-rich samples. There are peaks at about 170 cm^{-1} and 480 cm^{-1} which are due to first-order scattering of Si-Si vibrations in the transverse acoustical (TA) and transverse optical (TO) modes respectively. The TO mode is generally thought to reflect short distance order of the material and its peak width at 480 cm^{-1} is directly proportional to the mean bond angle aberration. The weak vibration band near 620 cm^{-1} corresponds to $Si\text{-}H_n$ wagging and the second-order longitudinal acoustic (LA) mode of Si-Si vibration. The weak 960 cm^{-1} band corresponds to the second-order transverse optic (TO) mode of Si-Si vibration. The weak band at 790 cm^{-1} is assigned to the Si-C vibration mode whose intensity (in their work) increases with carbon concentration. Yu *et al.* (2004) stated that the decrease in the number of amorphous silicon grains in the films with increasing carbon concentration can result in lower Raman scattering intensity.

Itoh *et al.* (2001) reported that they obtained hydrogenated amorphous silicon carbide (a-SiC:H) films with embedded silicon nanocrystallite by HW-CVD using CH_4 as a carbon source. They reported that in Raman spectra for the samples, peaks are found near 480 cm^{-1} and 520 cm^{-1}, which correspond to the amorphous silicon (a-Si) and crystalline silicon (c-Si) phases, respectively. The crystalline silicon carbide is not observed in the Raman spectra, therefore they concluded that the prepared samples have

a mixture of a hydrogenated amorphous silicon-carbon alloy (a-$Si_{1-y}C_y$:H) and hydrogenated microcrystalline silicon (μc-Si:H).

2.5 Studies on Optical Band Gap of Silicon Carbide

The optical band gap of the silicon carbide films prepared in this work was determined from the Tauc plot by extrapolating the linear part of the absorption versus photon energy (hυ) curve. Previous works reported that the optical band gap can be increased by increasing the carbon content in the films. However, a decrease in the optical band gap is also observed in high carbon content films, which is attributed to the formation of graphite-like carbon clusters (Pereyra and Carreno, 1996).

A variation in optical energy gap (E_{op}) from 2.0 to 2.6 eV was observed by changing the hydrogen flow assisting the deposition process from 0 to 300 sccm as reported by Park *et al.* (2001).

In an experiment done by Kumbhar *et al.* (2001), a-SiC:H films were deposited from a mixture of silane and acetylene gas by the cat-CVD technique. Their study showed that the acetylene to silane ratio (C_2H_2/ SiH_4) have affected the value of optical band gap and deposition rate under certain conditions of total gas pressure and filament temperature.

Kumbhar *et al.* (2001) also reported that the band gap is observed to increase gradually from 2.0 to 2.65 eV and then rapidly to 3.6 eV for the 0.8 C_2H_2 fraction. The initial increase in the band gap for C_2H_2 fraction less than 0.6 may be due to the substitution of Si-Si bonds, by Si-C, C-H and C-C strong bonds, while for C_2H_2 fraction greater than 0.6, the network becomes more carbon-rich, where the band gap is controlled by the formation of C-C and C-H bonds. It is believed that the increase in the band gap is due to the increase in the sp^3-bonded CH_n observed at 960 cm^{-1}.

Mori, Tabata and Mizutani (2006) focuses on the decomposition of methane molecules by using filament temperature above 2000°C and on the use of other molecules such as C_2H_2 and $SiH_x(CH_3)_{4-x}$ which are decomposed at a filament temperature below 2000°C. In another research work, their group (Tabata *et al.*, 2004) has succeeded in preparing a wide band gap a-$Si_{1-x}C_x$:H thin film using methane as a source gas even at a low filament temperature of 1400°C. It has been reported by other group (Matsuda, 1992) that high hydrogen dilution of source gases is important for the preparation of high quality a-$Si_{1-x}C_x$:H thin films in plasma enhanced CVD technique.

Mori, Tabata and Mizutani (2006) also investigated the influence of hydrogen gas flow rate on the properties of a-$Si_{1-x}C_x$:H thin films prepared by HW-CVD method. Their experiment showed no clear influence of H_2 flow rate (between 50-100 sccm) on the deposition rate of a-$Si_{1-x}C_x$:H thin films using HW-CVD technique. This is due to the small silane partial pressure. They also found that Si-CH_3 wagging mode (780 cm^{-1}) was pre-dominant in high energy gap a-$Si_{1-x}C_x$:H thin films. This suggests the high incorporation of carbon atoms into the films, resulting in optical energy gaps higher than 2.1 eV. On the other hand, the Si-H_n wagging mode peak (630 cm^{-1}) was as high as that of the Si-CH_3 wagging mode in the high energy gap group of a-$Si_{1-x}C_x$:H thin films. In both group of high and low energy gap, energy gap decreases with the increase in H_2 flow rate between 10 and 100 sccm.

DC magnetron sputtering technique was utilized to prepare a-$Si_{1-x}C_x$:H films by Keffous *et al.* (2010). They reported that the optical band gap value of the films increases from 2.0 eV with increase of the film thickness and reaches a constant value around 2.68 eV.

2.6 Application of Hot-Wire Filament in Chemical Vapor Deposition

Hot-Wire Chemical Vapor Deposition (HW-CVD) is a popular technique used in preparing silicon thin films such as hydrogenated amorphous silicon (a-Si:H) and hydrogenated microcrystalline silicon (μc-Si:H) at high deposition rate. This technique has been used extensively to produce diamond films (Wolden, Mitra and Gleason, 1992; Harris and Weiner, 1990), boron carbide coatings (Park *et al.*, 2001) cubic silicon carbide films (Kumbhar *et al.*, 2001) among others. Recent work reports the use of hot-wire plasma assisted CVD technique to produce amorphous and nanocrystalline silicon films (Rozhin *et al.*, 2002), to synthesize carbon nanotubes (Ying *et al.*, 2004) and to produce amorphous silicon carbide films (Chang and Sakai, 2004).

HW-CVD has important advantages of low-temperature and large area deposition. In addition, the HW-CVD has high gas-decomposition efficiency. It has been reported that the HW-CVD generates H radicals with a higher density than other thin film preparation techniques. It is recognized that high density H radicals is important for nanocrystalline growth at a low temperature (Matsuda, 2004). These suggest that the HW-CVD technique is suitable for low temperature growth of nanocrystalline cubic silicon carbide (nc-3C-SiC).

HW-CVD offers benefits such as higher deposition rates, lower hydrogen content films that show greater stability against light irradiation (Matsumura, 1998) and a relatively simple apparatus. Compared to PECVD, the method is also more conducive to modeling the deposition process and thus elucidating optimal parameters (Matsumura, 1998). In HW-CVD, the source gas is decomposed by a resistively heated metal filament at a temperature between 1750 and 1950^{o}C (for SiH_4) to produce film growth precursors which will affect the growth rate and film properties.

A wide range of hydrogenated amorphous silicon carbide (a-SiC:H) have been produced using HW-CVD technique with SiH_4, C_2H_2 and H_2 as the precursor gases (Swain and Dusane, 2006). a-Si:H were usually prepared by glow discharge or plasma-enhanced chemical vapor deposition (PECVD), or hot wire chemical vapor deposition (HW-CVD) technique. HW-CVD technique shows a lot of potential to replace the RF glow discharge method for the processing of all the silicon based amorphous alloy thin films such as a-Si:H, a-SiN:H, a-SiC:H and microcrystalline silicon (Swain and Dusane, 2006). The advantage of employing HW-CVD comes from the absence of the deterious electrons and ions and surface charges and also the high dissociation rate of source gases. The former relates to the avoiding of powder formation at high pressure and filament temperature and the latter leads to higher deposition rates (Mahan, 2003).

HW-CVD is a very effective technique for the deposition of device quality silicon thin films because this technique has the advantage of high deposition rate, low substrate temperature and large scale area deposition (Sugita *et al.*, 2003). However, it has been reported that in the HW-CVD method, it was difficult to prepare a-$Si_{1-x}C_x$:H thin films with a band gap above 2.0 eV using methane gas as the carbon source (Itoh *et al.*, 2001). It is believed that methane molecules are hardly decomposed on a tungsten wire heated at 1700^{o}C and that generation of methane related precursors is small (Schroeder, 2001).

2.7 The effects of filament temperature on the deposition process

Hot-wire filament is being used to enhance the growth of the film. The effect of heated filament in the plasma was primarily to increase the atomic hydrogen concentration in the plasma, thus improving the film properties. Indirectly, the heated filament is utilized to increase the carbon incorporation into the films in the favored

coordination, thus increasing the optical band gap of the films (Das, Chattopadhyay and Barua, 1998). For high filament temperature where the production of atomic hydrogen is expected to be higher, there could be a decrease in hydrogen coverage on account of rise in substrate temperature, thereby increasing the film deposition rate and deteriorating the film structure (Das, Chattopadhyay and Barua, 1998).

The downside of high growth temperatures is that sometimes it result in high tensile stress and crystalline lattice defects in the silicon carbide films due to the difference in thermal expansion coefficient between silicon and silicon carbide. Such defects and strain can degrade the carrier mobility and increase the junction leakage current. In order to widen its application to devices such as solar cells and thin film transistors, a low temperature deposition technique is desirable. Besides, the filament temperature is an important factor in determining the level of contamination and therefore the quality of the deposited film.

In the following are some reports done by other researchers regarding the utilizations of hot wire filament in the production of silicon carbide thin films. Ferreira *et al.* (1999) reported that nanocrystals start appearing for films prepared with filament temperature above 2173 K or 1900^{o}C using HW-CVD technique. Microstructure was enhanced as the filament temperature is increased from 1900 to 2000^{o}C. Martins (1998) previously reported that when the filament temperature increases from 1750 to 2050^{o}C, deposition rate increases. They also reported that at high filament temperatures, deposition rate decreased when hydrogen flow rate increased from 0 to 250 sccm.

Crystallinity could also occur in amorphous silicon carbide under certain circumstances. According to Ferreira *et al.* (1999), hydrogenated amorphous silicon carbide (a-SiC:H) films produced at high filament temperatures have a high degree of crystallinity. A minimum filament temperature of around 2000^{o}C is needed to promote

the nucleation of Si crystals. The same effect was observed with increase of hydrogen dilution (Ferreira *et al.,* 1999). Formation of larger SiC crystals was also reported by Joshi *et al.* (2009) due to higher plasma temperature and higher diffusion rate.

Doyle *et al.* (1988) used threshold ionization mass spectroscopy (TIMS) reported that below a filament temperature of 1400^{o}C, silane formed either a silicon film or silicide on the tungsten filament. Above 1100^{o}C, silicon and hydrogen atoms were observed to evolve, along with a much lower concentration of SiH_3. Alternative film growth precursors were suggested to be derived from film structure or from growth rate models. Gas phase reactions involving filament generated radicals are often believed to be major sources of growth precursors.

Negatively biased silicon substrates were also utilized in a PECVD system to facilitate the deposition of better crystalline and oriented β-SiC films at low temperature (Wang *et al.,* 2003). Hot-wire CVD is one of the most promising techniques for low temperature deposition of functional thin films (Matsumura, 1998; Chen *et al.,* 2009). It is widely recognized that high temperature (>1000^{o}C) are usually required for the fabrication of crystalline silicon carbide. However, it has also been reported that Si-crystallite-embedded a-SiC:H thin films were obtained under certain conditions. Recently, Tabata *et al.* (2009) reported findings which indicate that increase in filament temperature could enhance the growth of Si-crystallite which were embedded in a-$Si_{1-x}C_x$:H matrix.

Based on reports in the literature, Matsumura (1998) have proposed three temperature regimes, each producing different nascent precursor radicals. It has been noted that heating the filament beyond a certain temperature decreases the residence time of absorbed silane, which could potentially result in incomplete decomposition of the molecule, thus producing SiH_x fragments. However, the rate of silane decomposition

increases with filament temperature, so a faster reaction time may counter act a shorter residence time.

The species produced by the decomposition of silane on a hot tungsten filament at different temperatures are photo-ionized by 118 nm photons (Duan *et al.,* 2001). VUV photon generated at 118 nm (10.5 eV) is sufficiently energetic to ionize the radicals of interest, but generally not energetic enough to cause dissociative ionization. As the filament temperature is increased, the intensity of Si^+ begins to rise steeply at approximately 1300°C, while the intensities of SiH_3^+ and $Si_2H_6^+$ grow significantly only at higher temperatures. These results suggest that the filament must be at least 1300°C before useful film growing precursors are produced in significant quantities. Below this temperature, small amount of radicals may be produced but at levels near the spectral noise. It appears that silicon radicals (and presumably H) are the primary products over a temperature range of several hundred degrees, indicating that silane molecules hitting the filament are decomposed to near completion even in the lower hot wire temperature regime. At temperatures above 1800°C, however, the percentages of SiH_3^+ and $Si_2H_6^+$ increase steadily compared to Si^+ because Si production appears to approach saturation. Studies by Duan *et al.* (2001) suggest that the condition of the filament surface such as the presence of silicide, influences the production of Si_2H_6.

Nayak, Behera and Mishra (2011) produced silicon carbide nanorods directly from silicon carbide powder with effect of high temperature heat treatment. The powder was heated at 2700°C for 15 minutes by employing a typical configuration of arc Argon plasma. The problem of using methane as a carbon source in the preparation of silicon carbide thin films by HW-CVD is that the incorporation of carbon (C) atoms into the silicon carbide film is small and consequently the band gap of the resulting film is narrow and less than 2.0 eV. To circumvent this, some research groups have used a

filament temperature (T_f) above 2000°C which is higher than conventional T_f (1700-1800°C). Molecules such as C_2H_2 and $SiH_x(CH_3)_{4-x}$ were also chosen as an alternative to methane. Using high filament temperature should be avoided due to contamination from filaments and the constrain of filament lifetime (Matsumura, 1998, Itoh *et al.,* 2002)

The HW-CVD has high gas decomposition efficiency. It has been reported that the HW-CVD generates hydrogen radicals with a higher density than other thin film preparation techniques by 1 or 2 orders of magnitude. It is recognized that high-density H radicals is important for nanocrystalline growth at a low temperature (Matsuda, 2004). These suggest that the HW-CVD technique is suitable for low-temperature growth of nc-3C-SiC. It was found that the amount of Si-related radicals generated was quite larger than that of C-related radicals even when both the gas flow rate of silane and methane were 1.0 sccm.

2.8 The Influence of Source Gases

The source gases system play an important role with regards to the film composition and the film structure as well as properties. Swain and Dusane (2006) grew hydrogenated amorphous silicon carbide (a-SiC:H) on silicon substrates by HW-CVD technique, with hydrogen diluted mixtures of SiH_4 and C_2H_2 as the precursor gases. FTIR measurements from their work showed that with the increasing hydrogen flow rate, the relative intensity of C-H_n stretching/ wagging modes to that of Si-H_n stretching mode increases. There were low concentrations of C clusters in the C-rich a-SiC:H and low concentration of amorphous Si clusters in the Si-rich a-SiC:H thin films. The multiphase structure in the grown thin films should be in a small cluster size less than 1.0 nm. The as-deposited films show very smooth surface and suitable for integration in device structure, therefore grown a-SiC:H thin films could be used as protective

coatings in device (Swain and Dusane, 2006). Photoluminescence band centered at 1.63 eV was observed in the grown a-SiC:H films. The optical band gap was found to increase continuously with the increasing hydrogen flow rate. High intensity PL for all the a-SiC:H thin films were observed due to the increase of the probality of radiative recombination with the presence of clusters and the decrease of non-radiative recombination through defects. Both graphite-like phase and a-Si:H –like phase are light emitting grains. The two types of grains and Si-C network are the origin of the PL in hydrogenated a-SiC materials (Swain and Dusane, 2006).

Ethylene has lower dissociation efficiency in hot wire process than that of PECVD process (Ferreira *et al.,* 2001). Due to that, the presence of plasma is important for better carbon incorporation during the dissociation process, either for producing carbon or SiC films. However, ethylene is a good carbon source for controlling the band gap of a-SiC:H films produced by HW-CVD or PECVD techniques (Ferreira *et al.*, 2001). Higher optical band gap materials are obtained using lower percentages of ethylene in the gas mixture when compared to methane. HW-CVD technique also revealed the production of porous material, thus not suitable for optoelectronic (Ferreira *et al.,* 2001).

Analysis on the influence of ethylene percentage in the gas mixture and the hydrogen gas dilution on the properties of a-SiC:H films produced by HW-CVD, PECVD, (RF-PECVD films) an HWPA-CVD techniques was done by Ferreira *et al.* (2001). They suggested that deposition parameters such as gas pressure, carbon gas source, energy delivered to gas, gas flow rate and substrate temperature have great influence in the gas dissociation process, and therefore, in the way affects the amount of carbon incorporated in the film network. Effect of gas pressure was reported by Joshi *et al.* (2009) in their effort of producing carbon nanotubes from a silicon carbide

composite. They found that when the helium gas pressure in the chamber was increased, the crystal size of silicon carbide formed increases significantly.

2.9 Other related studies

Recently in South Korea, Lee, Jeon and Lee (2011) had successfully produced ultrananocrystalline diamond (UNCD) using direct-current plasma assisted chemical vapour deposition on silicon wafer using CH_4-H_2 and CH_4-Ar gases containing additive nitrogen. They demonstrated that the UNCD films were of excellent phase purity and its grain size were below 10 nm.

In coating technology, a group of Italian researcher (Zanella, Lekka and Bonora, 2009) used plating bath with galvanostatic deposition technique which was carried out under both direct-current (DC) and pulse current (PC) conditions. They studied the influence of the particle size on the mechanical and electrochemical behaviour of micro and nano-nickel matrix composite coatings. The minimum pulse current density of the was 0 while the maximum current density was maintained at 2 A dm^{-1} in order to compare the specimens with those produced under direct current.

Ellipsometry, FTIR, Raman and X-Ray Spectroscopy analysis were done on a-$Si_{1-x}C_x$:H film prepared by RF-PECVD by a group of researcher in China (Hong *et al.*, 2010). The PECVD chamber was equipped with RF power source with 13.56 MHz operating frequency. The chamber pressure was maintained at 7 x 10^{-4} Pa and 3 Pa during deposition. Annealing at elevated temperatures were done to the prepared samples. Results showed that the structural and optical properties of the a-$Si_{1-x}C_x$:H film can be effectively engineered by proper annealing conditions.

High voltage current was also utilized in pulsed laser ion implantation. In order to fabricate hydrogen detector based on an n-6H-SiC crystal, Fominskii *et al.* (2011) did

ion implantation of Platinum from pulsed laser plasma. During motion of plasma from the target to the substrate, a high voltage pulse with positive polarity was applied to the target holder. The amplitude of the pulse was 50 kV provided efficient acceleration of doubly charged ions from the laser plasma.